Iron-mediated C-C Bond Formation via Reductive Coupling with Carbon Dioxide

Tristan T. Adamson, Steven P. Kelley and Wesley H. Bernskoetter*

The Department of Chemistry, The University of Missouri, Columbia, Missouri, 65211, USA.

E-mail: bernskoetterwh@missouri.edu

Abstract

Carbon dioxide functionalization is a potentially transformative method to enhance the sustainability of carbon-based commercial chemicals. The reductive functionalization of CO_2 via C-C bond forming reactions is one route to deriving structurally diverse products from this renewable resource. Despite considerable advances in catalytic CO_2 reduction into smaller molecular fragments, such as CO, there remains relatively few transition metal mediated processes to elaborate CO_2 via reductive C-C bond functionalization. An investigation of iron(0) complexes capable of reductive coupling with CO_2 to generate acrylate and oxalate are described here. A set of [$(depe)_2Fe$] (depe = 1,2-bis(diethylphosphino)ethane) complexes were found to reductively functionalize CO_2 with ethylene or a second molecule of CO_2 to afford C_3 and C_2 products, respectively. Several factors influencing the stoichiometric yield of these transformations were examined including a deleterious CO_2 disproportionation process which produces $(depe)_2Fe(CO)$ and $(depe)_2Fe(CO_3)$. Additionally, an intermediate iron-lactone complex in route to acrylate formation has been structurally characterized.

Introduction

The abundant supply of carbon dioxide (CO_2) in earth's atmosphere represents a source of underutilized C_1 synthon that would offer great economic benefit if large-scale up-conversion processes were realized. Preliminary progress has been made towards this goal by numerous researchers, but greater advances in catalyst development are necessary before the full potential of carbon dioxide as a cheap source of carbon is achieved.[1] A plurality of recent research into CO_2 functionalization catalysts have pursued

thermochemical[2] and electrochemical[3] processes to make simple C_1 products, such as carbon monoxide (CO),[4,5] formic acid (HCOOH) or formate ($HCOO^-$),[6–8] methanol (CH_3OH),[9–11] and methane (CH_4).[12–14] While valuable, these targets offer limited chemical complexity. Expansion of the structural diversity of chemicals made via carbon dioxide functionalization will require catalytic reactions which form C-C bonds between CO_2 molecules or with other substrates. To date, the most oft-studied targets for catalytic reductive coupling of CO_2 include reactions to produce ethylene (C_2H_4)[15–17] or oxalate ($C_2O_4^{2-}$),[18–23] as well as the coupling of CO_2 and olefins to produce acrylate ($CH_2CHCO_2^-$)[24–32] or other carboxylates.[33,34]

Efficient oxalate (or oxalic acid, $H_2C_2O_4$) synthesis from CO_2 is a longstanding target for CO_2 functionalization, with moderately successful catalyst development appearing in the mid- 1990's.[18,19] Despite these efforts, most oxalate is commercially synthesized via the oxidation of carbohydrates or the coupling of carbon monoxide (CO) with alcohols under aerobic conditions.[1] Generating oxalate via CO_2 reduction has the potential to offer a more economical and atom-efficient alternative to these routes. A major challenge to CO_2 reductive coupling to produce oxalate is the endergonic reaction profile (-0.59 V vs SHE),[35] which requires that catalysts operate under an applied potential or in the presence of sacrificial reducing agents. Competitive reactions such as CO_2 insertion into metal hydrides or CO_2 disproportionation to CO and carbonate (CO_3^{2-}) can also pose potential selectivity issues.[18,20] Additionally, control of any highly reactive CO_2 radical anion ($CO_2^{\bullet-}$) intermediate formed during the reaction will impact feasibility. To date, a number of heterogeneous catalysts have been employed to facilitate this reaction, a leading example of which is a Cr-Ga oxide system capable of oxalate formation in water with a faradaic efficiency of 59%.[36] Only a handful of homogeneous catalysts exist, most of which are based on elaborate bi/tri-metallic complexes (Figure 1).[19–23] The highest turnover number (TON) reported under thermochemical reduction conditions thus far is 24, with a reduction yield of 95% facilitated by Murray's tricopper catalyst.[23] Electrochemical systems have seen greater activity, with Jäger's nickel catalyst facilitating a TON of up to 750 with 90% faradaic efficiency at a high overpotential (E_{cat} = -2.26 V SCE in MeCN).[20] Bouwman's bimetallic copper electrocatalyst selectively reduces CO_2 from air at an exceptionally low overpotential (-0.27 V vs SCE), but suffers from the need for lithium salt additives to promote dissociation

of oxalate from the copper complex, as well as a low TON of 12.[21] Despite the excellent progress made by these previous investigations, significant advances in catalyst development are required to achieve well-understood, industrially relevant systems for CO_2 to oxalate conversion.

In addition to CO_2 homocoupling, the transition metal-catalyzed coupling of CO_2 and C_2H_4 to form acrylic acid (or acrylate) offers an alternative route to creating more elaborate products from CO_2 functionalization. Acrylic acid and its derivatives are currently prepared via fossil fuel sourced propylene oxidation and serve as valuable commercial chemicals used in the manufacturing of paints, adhesives, superabsorbent polymers, and other materials.[1,24] A commonly proposed reaction mechanism for transition metal-mediated acrylate formation from CO_2 and C_2H_4 is provided in Figure 2.[37] Although Hoberg and coworkers published the first example of CO_2/C_2H_4 coupling to metal-lactones nearly 40 years ago,[38] an industrially relevant catalyst for acrylic acid synthesis from CO_2 has not yet been realized. One challenge is the unfavorable thermodynamic profile of the reaction ($\Delta G° = +42.7$ kJ/mol).[39] This has traditionally been overcome via the addition of stoichiometric base to form the more stable sodium acrylate salt ($\Delta G = -59$ kJ/mol).[37] Nickel-based catalysts are the most extensively studied systems to date, with the highest TONs ranging from 400-450 (Figure 3).[30,40] However, many nickel systems require specialty bases and excess stoichiometric additives, such as zinc dust and Lewis acid, where the interplay of the multiple reaction components is not well understood.[30] Limited advance in the TONs achieved by extensive empirical optimization of current nickel systems suggests alternate classes of catalysts should also be explored.

Consideration of the prior art for reductive CO_2 coupling to oxalate and acrylate (*vide supra*) suggests some similarities in catalyst design criteria for both reactions. A potential CO_2 to oxalate catalyst must be highly electron rich in order to achieve CO_2 reduction/coupling at a reasonable rate,[20] and the transition metal center must have a low oxophilicity and Lewis acidity to avoid strong oxalate coordination, which has limited some previous catalyst investigations.[21,22] As evidenced by the monometallic nickel catalyst developed by Jäger,[20] elaborate bi/tri-metallic complexes are not required for achieving oxalate formation, despite this feature being common in several examples. For a CO_2 to acrylate catalyst target to

be viable, the complex must likewise be highly electron rich to provide enough reducing potential for the initial cyclization reaction. The catalyst target must also have a low oxophilicity to allow release of free acrylate, which has previously limited potential catalysis on molybdenum and tungsten.[41,42] Finally, acrylate catalysts must be capable of β-hydride elimination from the lactone intermediate. This step has proven limiting for square planar nickel-lactones (Figure 2) because of the inability of the structure to reach an agostic intermediate. This limitation likely originates from the only unoccupied metal *d*-orbital lying in the plane of the ligands where it is inaccessible.[25] Thus, we hypothesized that pursuing a metal-lactone intermediate with a *d*-electron count of ≤ 6 would be advantageous.

Drawing on these design criteria, we hypothesized that the previously characterized iron(0) complexes of the type $(depe)_2Fe(L)$ (depe = 1,2-bis(diethylphosphino)ethane), where L = C_2H_4[43] or CO_2,[44] would be promising targets for the synthesis of both acrylate and oxalate from CO_2. Herein, we report the first well-defined example of iron-mediated acrylate formation from CO_2-C_2H_4 coupling, as well as a fully characterized iron-lactone intermediate arising from the coupling reaction. This same system is also capable of stoichiometric oxalate production in near quantitative yield in a thermochemical reaction using a sacrificial one-electron reductant.

Introduction Figures

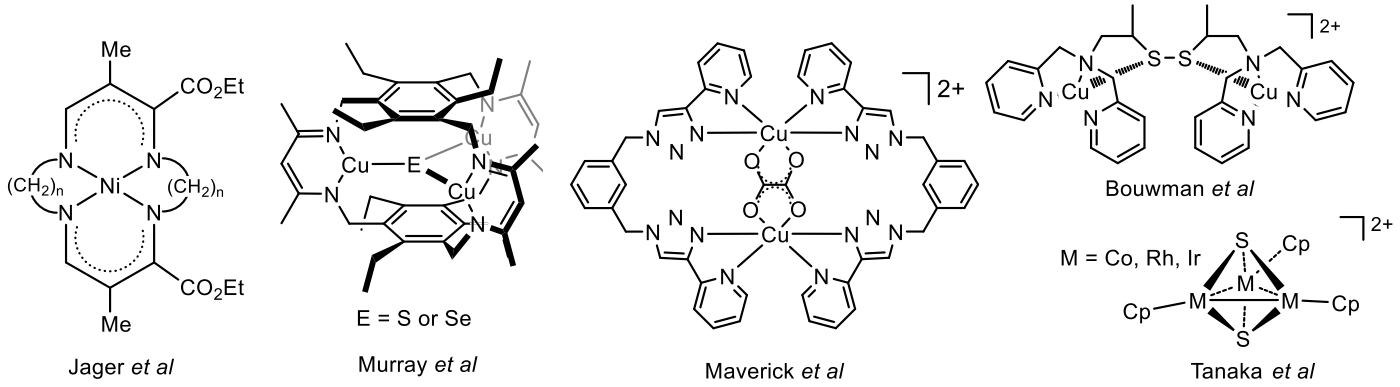

Figure 1. Previously reported homogeneous catalysts for CO_2 to oxalate conversion.

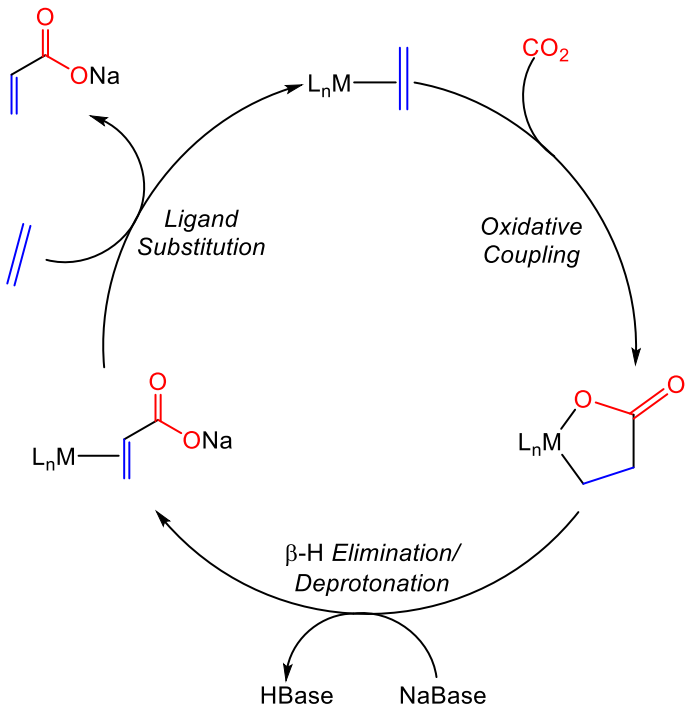

Figure 2. Postulated mechanism for transition metal mediated CO_2-C_2H_4 coupling to produce acrylate.

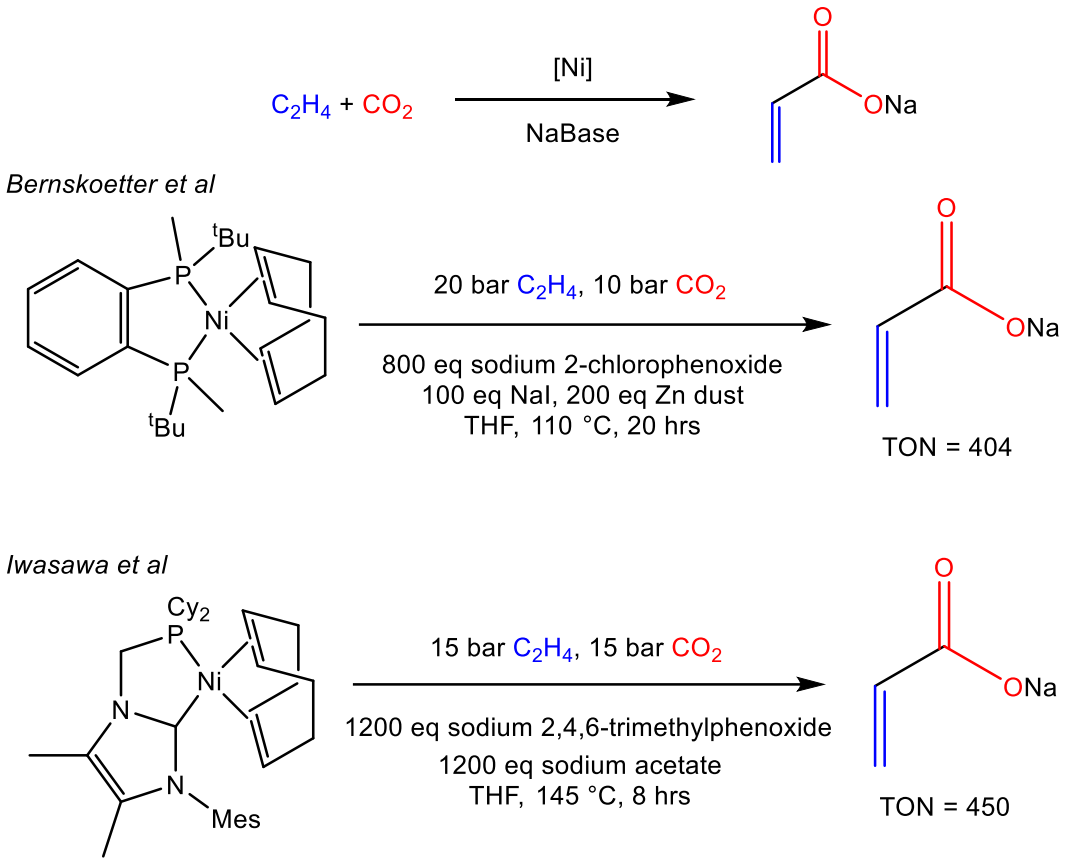

Figure 3. Leading catalysts for CO_2-C_2H_4 coupling to produce acrylate.

Results and Discussion

Acrylate Formation Studies

Initial efforts focused on the synthesis of the CO_2-bound iron complex $(depe)_2Fe(CO_2)$ (**1**) using a previously published procedure.[44] Potassium graphite (KC_8) reduction of the iron dichloride complex, $(depe)_2FeCl_2$,[45] under a dinitrogen atmosphere over three days resulted in formation of the iron(0) species $(depe)_2Fe(N_2)$ (**2**) as an orange solid in good yield.[46,47] Prolonged reaction times were necessary to fully convert partially reduced iron(I) impurities. Subsequent treatment of **2** with 1 equiv of CO_2 afforded clean conversion to **1**.[44] Attempted CO_2-C_2H_4 coupling was performed by adding 3 equiv of $^{13}CO_2$ and 3 equiv C_2H_4 to a C_6D_6 solution of $(depe)_2Fe(^{13}CO_2)$ (**1-$^{13}CO_2$**) in an NMR tube at ambient temperature. Monitoring the reaction by ^{13}C NMR spectroscopy over 24 hours revealed two enhanced resonances of roughly equal

intensity at δ 224.5 and 164.8 ppm, which were assigned to the carbonyl, $(depe)_2Fe(CO)$ (**3**), and the carbonate, $(depe)_2Fe(CO_3)$ (**4**) complexes respectively (Figure 4). The identity of **3** and **4** were confirmed by comparison to spectra from authentic samples prepared via alternate methods.[44,48,49] These species presumably arise from CO_2 disproportionation, a reaction commonly reported in iron mediated CO_2 reduction chemistry.[49–51] It is hypothesized that the strong electron donating ability of **1** imparts nucleophilic character to the bound CO_2 and permits attack on a free or activated CO_2 molecule to start a pathway that leads to reductive CO_2 disproportionation.[49,50] However, most prior examples of CO_2-C_2H_4 coupling employ complexes with ethylene already bound to the metal center (Figure 5). For instance, the first example of iron-mediated CO_2-C_2H_4 coupling reported by Hoberg and coworkers in 1987 produced succinic and methylmalonic acid derivatives by insertion of multiple CO_2 molecules into $(PEt_3)_2Fe(C_2H_4)_2$ (Figure 5a).[33] More recently, Chirik and coworkers reported a pyridine(diimine) iron dinitrogen complex that couples CO_2 with a varying number of C_2H_4 units to produce saturated and unsaturated carboxylates (Figure 5b).[34] Notably, it was reported that when CO_2 was charged before C_2H_4, no desired coupling reaction was observed, analogous to the behavior of **1**. While these prior works indicate that selective iron-mediated acrylate formation from CO_2 and C_2H_4 should be feasible, no well-defined examples have yet been reported.

Given the precedents for CO_2-C_2H_4 coupling at iron-ethylene complexes, we next examined the reactivity of $(depe)_2Fe(C_2H_4)$ (**5**).[43] Complex **5** was first generated *in situ* by placing **2** under 6 equiv C_2H_4 at ambient temperature in C_6D_6 overnight. ^{31}P NMR spectroscopy indicated partial conversion to **5** had occurred, with about 50% of **2** remaining. Subsequent addition of 3 equiv $^{13}CO_2$ to this sample without removing the gaseous C_2H_4 produced three new enhanced resonances in the ^{13}C NMR spectrum at δ 224.5, 189.2, and 164.8 ppm over 2 days at ambient temperature. The peaks at δ 224.5 and 164.8 ppm were again assigned to the CO_2 disproportionation products **3** and **4**, which in this case arise after ligand substitution of **5** (or residual **2**) with CO_2 affords complex **1** (Figure 4). Alternatively, the ^{13}C NMR resonance at δ 189.2 ppm appears to result from coupling of $^{13}CO_2$ with the bound ethylene to afford $(depe)_2Fe(\kappa C,\kappa O\text{-}CH_2CH_2{}^{13}COO)$ (**6-$^{13}CO_2$**) (Figure 4). Treatment of **6-$^{13}CO_2$** with HCl produced ^{13}C-labelled propionic acid

which was identified by ^{1}H-^{13}C HMBC NMR analysis and comparison to authentic samples. Additionally, the ^{13}C NMR resonance at δ 189.2 ppm was correlated to two ^{1}H NMR signals at 1.94 and 2.84 ppm via 2D ^{1}H-^{13}C HMBC NMR spectra, consistent with C-C bond formation between the CO_2 and ethylene fragments.

The observation of **6-$^{13}CO_2$** from *in situ* NMR spectroscopy experiments was encouraging, but to slow the rate of deleterious CO_2 disproportionation and more selectively generate the lactone complex, isolated samples of **5** were prepared by KC_8 reduction of $(depe)_2FeCl_2$ under ethylene atmosphere. Although alternative preparation methods of **5** have been reported previously,[52] x-ray diffraction data was obtained that solidified its characterization (Figure 6). The iron-ethylene adduct crystallized in a relatively symmetric orthorhombic space group with a 2-fold axis bisecting the ethylene C-C bond. The complete molecule of **5** illustrated in Figure 6 is thus generated by symmetry with the C(11)-C(11A) distance of 1.432(2) Å suggesting a high degree of back-bonding from the electron rich metal center.[53] Conveniently, exposure of samples of **5** to an atmosphere of dinitrogen in either the solid state or solution did not result in any conversion to **2**, enabling handling in a glovebox. Compound **5** was treated with 6 equiv C_2H_4 and 3 equiv $^{13}CO_2$ at ambient temperature in order to minimize the amount of **1** formed. This procedure led to selective formation of **6-$^{13}CO_2$** overnight with no evidence of CO_2 disproportionation products in the ^{13}C or ^{31}P NMR spectra. Recrystallization of unlabeled $(depe)_2Fe(\kappa C,\kappa O\text{-}CH_2CH_2COO)$ (**6**) in diethyl ether led to red crystals suitable for analysis by x-ray diffraction. The solid-state structure of **6** is provided in Figure 6. The data reveal an approximate octahedral coordination environment featuring a five-membered metal-lactone ring. The metallocycle is relatively planar with an O(1)-Fe(1)-C(21)-C(22) torsion angle of 13.56(9)°. Additionally, the C(23)-O(1) and C(23)-O(2) bond lengths of 1.291(2) and 1.241(2) indicated partial delocalization of the carboxylate π-bond. Iron metallocycles related to **6** have been previously studied by x-ray diffraction,[54,55] though **6** is the first parent lactone derived from CO_2-ethylene coupling to be structurally characterized.

Complex **6** proved highly resistant to β-hydride elimination to yield an acrylate species even upon heating to *ca* 90 °C, above which decomposition occurred to a mixture of **3**, free ligand and free ethylene.

The stability of **6** is likely due to its 18-electron configuration and the absence of a labile ligand which blocks the intramolecular β-hydride elimination process.[25] In an attempt to determine the stability of any transiently formed iron acrylate hydride species, 1 equivalent of acrylic acid was added to a sample of $(depe)_2Fe(N_2)$, which produced *trans*-$(depe)_2Fe(H)(\kappa O\text{-}O_2CCH{=}CH_2)$ (**7**) (Figure 7). The ^1H NMR spectrum of **7** contains a metal-hydride quintet at -33.16 ppm, and the proton decoupled ^{31}P NMR spectrum contains one resonance at δ 89.95 ppm, consistent with four equivalent phosphorous nuclei. The solid-state structure of **7** obtained from X-ray diffraction experiments is provided in Figure 6. Unfortunately, the preparation of **7** offers little insight into the kinetic or thermodynamic accessibility of an iron acrylate hydride species produced by β-H elimination from **6** because of its *trans* configuration (Figure 7). Only the *cis* isomer should be produced kinetically from β-hydride elimination of **6**, and it is unknown if the *trans* isomer **7** is kinetically and/or thermodynamically selected from the protonation reaction. Coincidentally, heating of complex **7** up to *ca* 90 °C produced no evidence for conversion to **6** and no isomerization to an alternative *cis* isomer was observed before significant sample degradation occurred.

One strategy to overcome the difficulty of β-hydride elimination from nickel-lactone species has been the use of Lewis acid additives in combination with mild Brønsted bases.[25,30,56,57] Interaction between the Lewis acid and the electronegative oxygen atoms is thought to allow transient ring opening of the lactone, creating a vacant coordination site on the metal as well as alleviating the rigid ring structure and facilitating access to the β-hydrogens.[25,56] Alternatively, stronger Brønsted bases may be used to directly deprotonate a C-H adjacent to the lactone carbonyl, permitting elimination to an acrylate ligand.[58] Unfortunately, the use of strong base is often incompatible with the presence of excess CO_2 owing to the formation of alkylcarbonates.[32,57]

In an attempt to promote acrylate formation, a C_6D_6 solution of **6** was treated with 5 equiv of the Lewis acidic lithium triflate (LiOTf) salt and 5 equiv of sodium 3-flourophenoxide. Upon heating overnight at 60 °C, a significant amount of insoluble salt formed in the NMR tube. ^1H NMR spectra of this material in D_2O confirmed the formation of sodium acrylate. The importance of Lewis acid was demonstrated by performing the same experiment with no LiOTf present which yielded no observable acrylate by ^1H NMR

spectroscopy. Likewise, acrylate production was also obtained by the addition of a strong base, sodium ^{t}butoxide (NaO^{t}Bu), to **6** in the absence of Lewis acid additives while heating overnight at 50 °C. However, reaction of **6** under these conditions with sodium 3-flourophenoxide or sodium 2,6-diisopropylphenoxide produced no detectable acrylate.

Given the ability of **5** to react with CO_2 to produce (sub)stoichiometric levels of acrylate in NMR-scale experiments under moderate basic conditions, we next tested the ability of this complex to generate acrylate catalytically. A wide variety of conditions were attempted, based on previously optimized nickel catalyst studies (see supporting information).[30,32] The only set of conditions that produced even sub-stoichiometric acrylate was when the strong base NaO^{t}Bu was employed. The inability of this complex to operate catalytically is likely due to its 18-electron configuration, and the associated difficulty with undergoing β-hydride elimination from an electronically saturated species. Given that all ligands in this system are chelating, transient formation of a long-lived open coordination site would be challenging. In the near future, we hope to target novel, electron-rich iron complexes which will provide this coordination environment.

Oxalate Formation Studies

Having found the $\{(depe)_2Fe^0\}$ fragment capable of reductive C-C bond coupling with CO_2 and C_2H_4, its competency in oxalate formation was investigated. Complex **1** was initially targeted because in addition to the design criteria given above, this complex is among only a limited number of isolable transition metal CO_2 complexes, and this stable pre-coordination may improve the selectivity of reduction.[50,59–64] Furthermore, the bending of the CO_2 bond angle upon coordination could lower the potential required for 1-electron reduction (E^0 = -1.90 V vs NHE) by alleviating the degree of reorganization required in the transition structure.[65] To date, iron-mediated oxalate formation reactions have been exclusively seen at iron(I) complexes. For example, a dibenzotetramethyltetraaza[14]annulene iron(I) complex was shown to react with CO_2 in toluene to produce limited sodium oxalate, but in THF reductive disproportionation dominated the product mixture.[51] In 2013, Peters and co-workers showed that a trisphosphino-borate iron(I) complex was capable of converting CO_2 into a bridging oxalate ligand in up to

70% yield. This yield was maximized following an elegant mechanistic study which showed that coordinating solvents or capping phosphine ligands were key to achieving CO_2 reductive coupling instead of reductive disproportionation (*vide infra*).[66]

Cyclic voltammetry (CV) experiments were initially performed on **1** to identify its potential as a CO_2 reduction electrocatalyst. In a 0.1 M THF solution of tetrabutylammonium hexaflourophosphate ($TBAPF_6$) under 1 atm argon, the first reduction wave of **1** does not begin until a potential of about -2.8 V (vs dFc^0/dFc^+) (see supporting information). Unfortunately, this runs counter to our hypothesis that the reduced CO_2 bond angle in this complex would ease the reduction potential. In fact, under these conditions the glassy carbon working electrode readily reduces CO_2 on its own. The highly cathodic reduction potential may originate from the highly reduced state of the iron center. Furthermore, when the electrochemical cell is purged and saturated with CO_2, the color of the solution quickly changes from a dark red to a bright yellow color, which is accompanied with complete degradation of **1** to **3** and **4**, as evidenced by CV and ^{31}P NMR analysis of the yellow solution.

It was apparent that electrocatalytic reduction of **1** was not a feasible route to oxalate formation, so focus was shifted to thermochemical reduction methods. Due to the high reduction potential of **1** observed during CV experiments, KC_8 was chosen for its strong reduction potential and its prior use in thermochemical oxalate catalyst studies.[23] Initial examinations employed the ^{13}C-labelled complex **1-$^{13}CO_2$** which was synthesized in an analogous fashion to the unlabeled complex using $^{13}CO_2$. **1-$^{13}CO_2$** was treated with 7 equivalents KC_8 and 10 equivalents $^{13}CO_2$ in THF over a period of 24 hours, after which the reaction was quenched with dilute HCl to liberate all oxalate as free acid and to eliminate any carbonate that may have formed. After separation of the organic material with diethyl ether, ^{13}C NMR analysis was performed on the aqueous layer. One single enhanced resonance was observed in the ^{13}C NMR spectrum at 164.5 ppm, consistent with a spectrum of an authentic oxalic acid sample. A control experiment conducted under the same conditions but omitting the iron complex did not produce any observable ^{13}C NMR resonances in this region, suggesting that the presence of **1** was important for oxalate formation. Likewise, no observable

oxalate production occurred when the same reaction was carried out in the absence of reducing agent, eliminating any solely iron(0) based reaction in the formation of oxalate.

Based on this preliminary success, efforts turned toward quantifying the oxalate production in this system. Using a technique previously reported for the analysis of oxalate yield, the post-reaction components were separated and the remaining aqueous oxalic acid solution titrated with 0.1 M potassium permanganate ($KMnO_4$).[20,67] Under the initial set of conditions, where 0.02 mmol **1**, 20 equivalents KC_8, and 1.5 atm CO_2 were charged in 15 mL THF at ambient temperature, an average conversion of 1.48 equiv of oxalate per iron was observed over a 20 hour period. Screening a variety of reaction conditions (see Supporting Information), including altering solvent, CO_2 pressure, reducing agent equivalents, catalyst loading, and temperature did not result in any significant improvements in activity. The highest conversion for oxalate under any set of conditions was 2.15 equiv. of oxalate per iron, during which 40 equivalents of KC_8 were employed. This represents a disappointing 10.9% reduction yield and within the uncertainly values of the analysis may not even be considered catalytic. Furthermore, a control experiment demonstrated that under these forcing conditions over half of the oxalate produced was a result of direct KC_8 reduction.

The lack of success seen during catalysis attempts turned efforts towards optimizing the system as a stoichiometric reaction. By lowering the KC_8 loading to only 2 equiv per iron and conducting the reaction under 1.5 atm CO_2 in THF at ambient temperature, a 79.5% oxalate yield was observed. Heating the reaction to 45 °C afforded an excellent yield of 98.1% (Table 1; entry 1). Under these conditions, the reduction yield of the KC_8-only control was only 15.8% (entry 8). The analogous iron(0) dinitrogen and carbon monoxide complexes **2** and **3** were shown to be nearly as active as **1** under these conditions (entries 2,3), suggesting the $\{(depe)_2Fe^0\}$ fragment is largely responsible for the reductive CO_2 coupling. This is supported by the observation that neither an alternative iron(0) source, ($Fe(CO)_5$; entry 5) nor a (depe)iron(II) source (entries 4 & 6) were capable of achieving high-efficiency oxalate production under these conditions. Similarly, $FeCl_2$ alone was shown to be ineffective for CO_2 coupling (entry 7). So, while

not a strong catalytic system, these experiments indicate **1** or similar iron(0) species have the potential to be efficient at CO_2 reductive coupling.

To better understand why the $\{(depe)_2Fe^0\}$ system is incapable of catalysis despite the high stoichiometric efficiency, a post-reduction mixture from an optimized stoichiometric trial was analyzed by ^{31}P NMR spectroscopy. In addition to small amounts of free ligand, a singlet at δ 87.1 ppm and two triplet resonances at δ 80.7 and δ 71.0 ppm were observed, consistent with formation of **3** and **4**, respectively. These observations indicate that CO_2 reductive coupling to oxalate is hindered by the competitive CO_2 disproportionation reaction (Figure 8). It appears that as disproportionation occurs and the iron(II) complex **4** is formed, the needed iron(0) is diminished over time. Additionally, any reduction of **4** back to iron(0) may contribute to a competitive cycle that consumes the reductant but produces carbonate. Both circumstances would lead to less efficient oxalate production as the reaction progresses. Based on these findings, it is possible that the efficient stoichiometric oxalate formation in this system is not the result of a highly selective iron-mediated reaction; rather, some iron(0) molecules produce several equivalents of oxalate, while others follow a deleterious CO_2 disproportionation pathway. Unfortunately, the addition of greater amounts of CO_2 or reducing agent to aid catalysis does not appear to favor the oxalate pathway, thus limiting the reaction to a modest conversion. Designing alternative iron complexes that limit preference for CO_2 disproportionation by reducing nucleophilicity of the bound CO_2 or impeding bimolecular reactions may be a productive line of investigation.

Concluding Remarks

The $\{(depe)_2Fe^0\}$ fragment has been demonstrated to be a versatile organometallic mediator of CO_2 reductive coupling to form C-C bonds. In the case of $(depe)_2Fe(C_2H_4)$, reaction with CO_2 to produce a metallalactone is facile, occurring at room temperature. However, the difficulty of β-hydride elimination from the electronically saturated species appears to limit capacity for catalytic acrylate formation. It is apparent that an effective iron-based catalyst for CO_2-C_2H_4 coupling must be able to reach a transient 16-electron state and work is continuing in our laboratory to design such a complex. The $\{(depe)_2Fe^0\}$ fragment also mediates the one-electron reduction of CO_2 to form oxalate with high efficiency but fails to perform

catalytically due to a competitive CO_2 disproportionation pathway. Based on the proposed mechanism for CO_2 disproportionation in these systems,[49] this pathway may be disfavored if the bound CO_2 is less nucleophilic. This could be accomplished by a metal center that is less electron rich yet still sufficiently reducing to promote a one-electron transfer to an activated CO_2 fragment. Therefore, an iron-based CO_2 to oxalate catalyst will require a delicate electronic balance, and work is ongoing in our laboratory to perform ligand alterations that meet these criteria.

Figures for Results Section

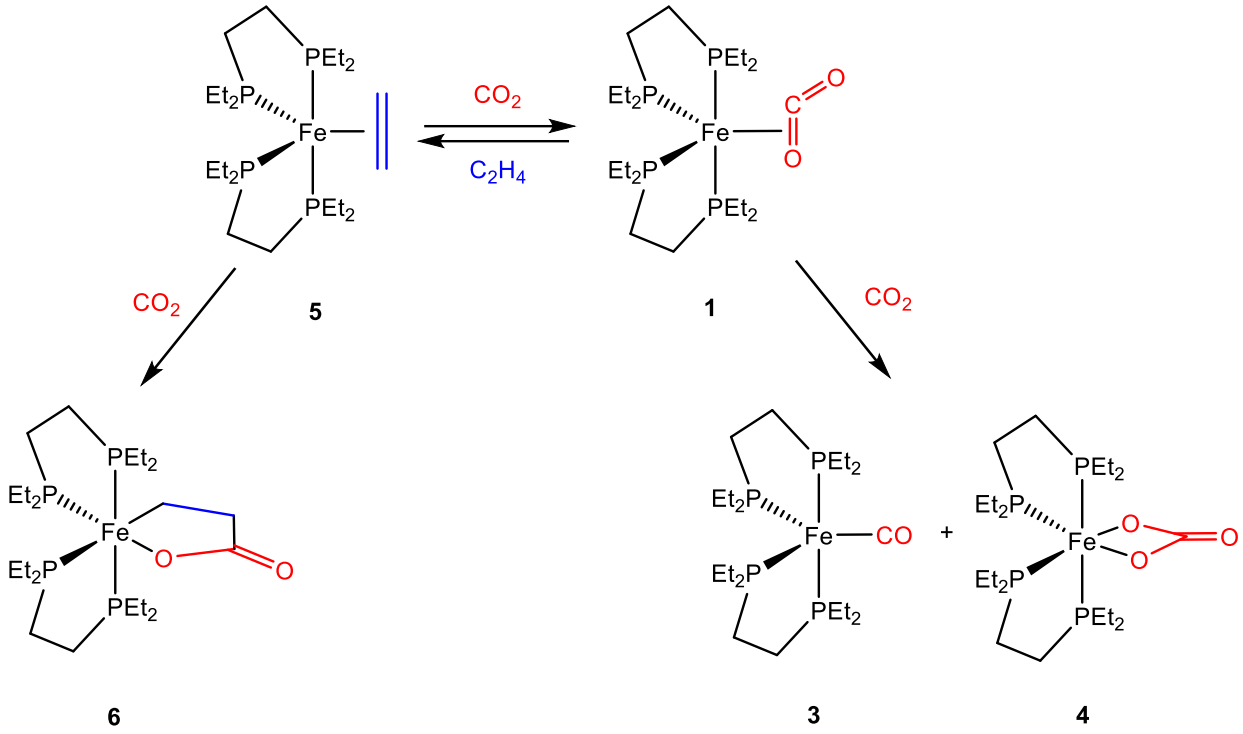

Figure 4. Competitive reaction pathways of lactone formation (left) vs reductive disproportionation (right).

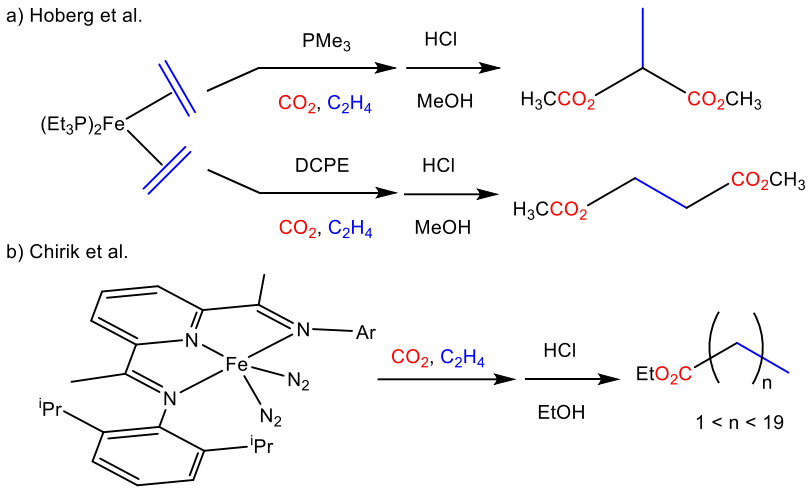

Figure 5. Previous examples of iron-mediated CO_2-C_2H_4 coupling. DCPE = 1,2-bis(dicyclohexylphosphino)ethane.

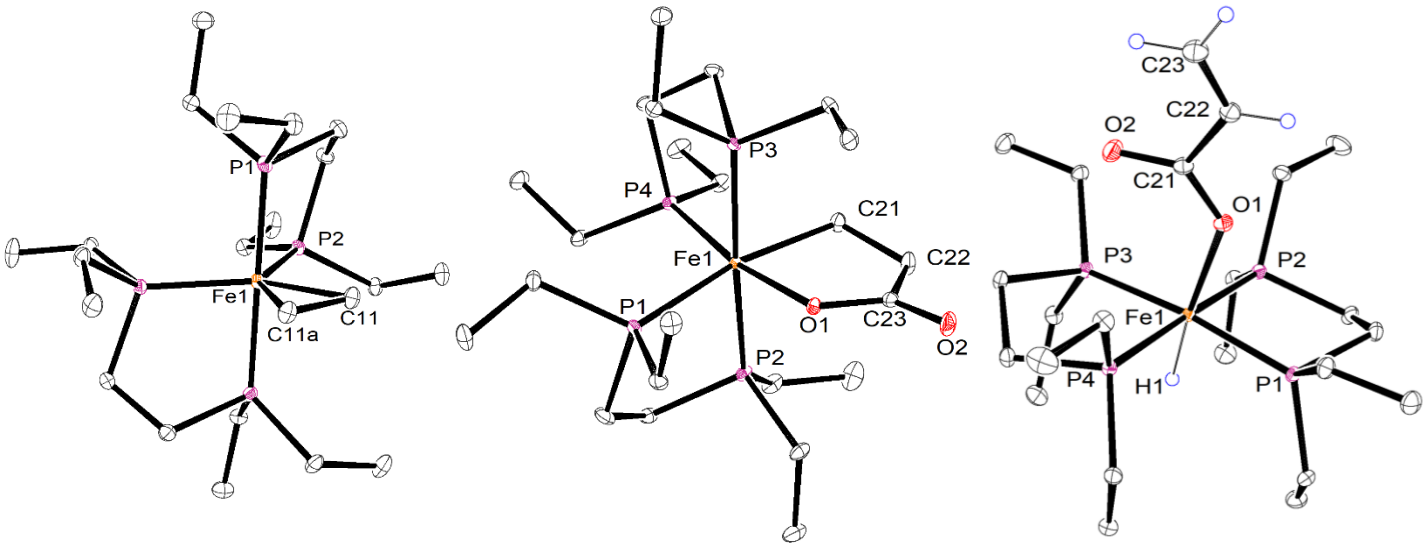

Figure 6. Molecular structure of **5** (left), **6** (center) and **7** (right) at 30% ellipsoids. All hydrogen atoms expect those attached to iron or acrylate have been removed for clarity.

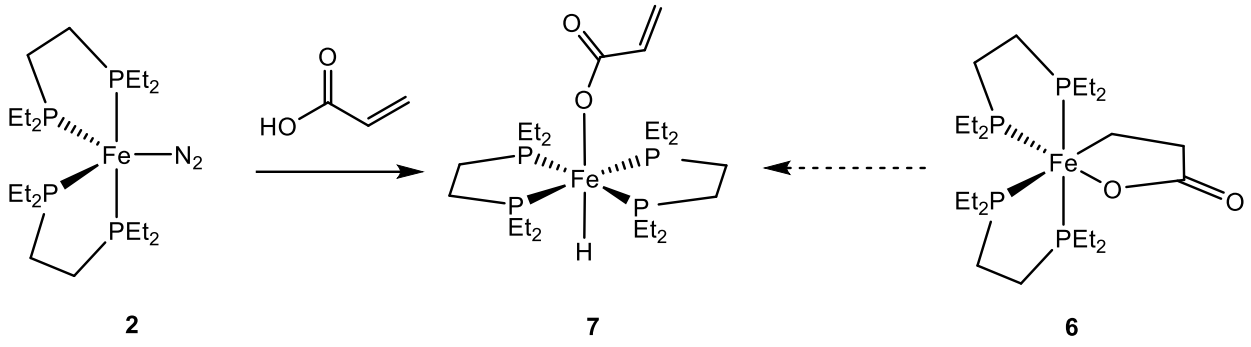

Figure 7. Protonation of complex **2** by acrylic acid to generate **7** and the unobserved β-H elimination route from **6.**

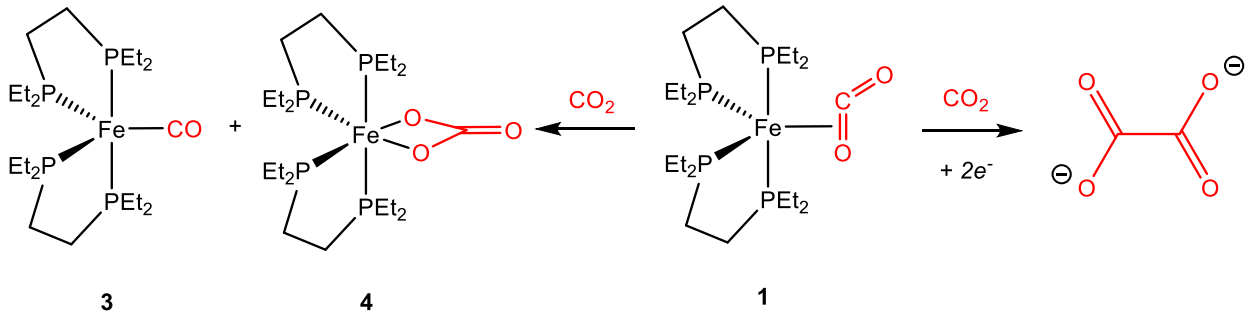

Figure 8. Competitive reaction pathways of oxalate formation and reductive disproportionation from **1**.

Table 1. Oxalate Production from Iron Complexes[a]

Entry	Complex	Yield (%)[b]
1	$(depe)_2Fe(CO_2)$ (**1**)	98.1 ± 2.1
2	$(depe)_2Fe(N_2)$ (**2**)	90.5 ± 9.1
3	$(depe)_2Fe(CO)$ (**3**)	87.5 ± 9.6
4	$(depe)_2Fe(CO_3)$ (**4**)	43.7 ± 6.9
5	$Fe(CO)_5$	16.6 ± 4.7
6	$(depe)_2FeCl_2$	24.1 ± 6.7
7	$FeCl_2$	17.7 ± 4.6
8	KC_8 Only	15.8 ± 5.4[c]

[a] Conditions: In all trials, 0.02 mmol {$(depe)_2Fe$}, 0.04 mmol KC_8, and 1.5 atm CO_2 in 15 mL THF solution for 24 hours at 45 °C. [b] Percent yields are reported with respect to [Fe]. Each is an average of three replicates followed by standard deviation. [c] Percent yield for this entry reported with respect to 2 equiv. of KC_8 per oxalate.

Experimental

General Experimental Procedures*:* All work was performed using standard air-free vacuum, Schlenk, cannula, and glovebox techniques. All chemicals were purchased from Aldrich, Alfa Aesar, VWR, Strem, or Fischer; isotopically enriched chemicals were purchased from Cambridge Isotope Laboratories. $(depe)_2FeCl_2$,[45] $(depe)_2Fe(CO_2)$ (**1**),[44] $(depe)_2Fe(N_2)$ (**2**),[47] $(depe)_2Fe(CO)$ (**3**),[44] $(depe)_2Fe(CO_3)$ (**4**),[48] and KC_8[68] were synthesized according to the literature procedures. Depe (98%) was used as received. Phenoxide bases were prepared by reaction of sodium hydride with the corresponding phenol derivative.[32] Solvents were dried and degassed according to the literature procedures.[69] 99.8% carbon dioxide, and dry ethylene were used as received from Airgas. All NMR spectra were recorded on Bruker 300 MHz DRX, 500 MHz DRX, or 600 MHz spectrometers. ^1H and ^{13}C NMR spectra were referenced to solvent signals, while ^{31}P NMR spectra were referenced to 85% phosphoric acid external standard. Acrylate catalytic trials were performed in a Parr 5500 series compact reactor with a glass insert. X-ray crystallographic data were collected on a Bruker SMART CCD system. Samples were collected in inert oil and quickly transferred to a cold gas stream. The structures were solved from direct methods and Fourier syntheses and refined by full-matrix least-squares procedures with anisotropic thermal parameters for all non-hydrogen atoms. *Electrochemistry:* Cyclic voltammetry experiments were conducted using a Gamry Interface 1010B potentiostat. A glass cell from Adams and Chittenden was employed with a three

electrode system which consisted of a 0.071 cm^2 glassy carbon working electrode, a non-aqueous $Ag/AgNO_3$ reference electrode, and a coiled platinum counter electrode which was kept in a separate compartment behind a porous frit. Positive scan polarity was employed with a scan rate of 100 mV/s. 2 mM analyte was used in a 0.1 M tetrabutylammonium hexaflourophosphate THF solution. Decamethyl ferrocene (dFc) was used as an internal standard, and potentials were referenced by placing the dFc^+/dFc^0 wave at 0.0 V.[70]

Synthesis of $(depe)_2Fe(C_2H_4)$ (5). This complex was synthesized according to a procedure modified from a previous report.[43] To a 50 mL heavy walled glass reaction vessel, 205 mg (0.380 mmol) $(depe)_2FeCl_2$ and 154 mg (1.14 mmol) KC_8 were added. The flask was cooled with liquid nitrogen and evacuated. THF (15 mL) was vacuum transferred to the flask. Without allowing the flask to warm up, 2.28 mmol ethylene was added via a calibrated gas bulb. The reaction was stirred at ambient temperature overnight. The volatiles were removed in vacuo before dissolving the residue in pentane and filtering through Celite. The filtrate was slightly concentrated before recrystallizing at -35 °C overnight. Yellow crystals of $(depe)_2Fe(C_2H_4)$ were isolated in 73% yield (137 mg). The identity of the product was initially verified by comparison with the literature values.[43] Additional characterization: ^{13}C $\{^1H\}$ NMR (600 MHz, C_6D_6): δ 26.5 (p, J = 13.2 Hz, Fe-α-CH_2), following signals assigned as P-CH_2 and P-CH_3 of depe ligand: 32.3 (br s), 29.6 (t, J = 9.7 Hz), 23.5 – 23.1 (m), 15.1 (m), 10.0 (s), 9.9 (br s), 9.4 (br s), 8.5 (br s), multiple resonances assumed to correspond to coincident carbons.

Synthesis of $(depe)_2Fe(\kappa C,\kappa O\text{-}CH_2CH_2COO)$ (6). To a 50 mL heavy walled glass reaction vessel, 92 mg (0.185 mmol) $(depe)_2Fe(C_2H_4)$ and 15 mL tetrahydrofuran were added. 1.48 mmol of ethylene and 0.741 mmol carbon dioxide were added via a calibrated gas bulb and the reaction allowed to stir at ambient temperature overnight. Volatiles were removed in vacuo before dissolving the residue in diethyl ether and filtering through micro-glass filters. The filtrate was slightly condensed before recrystallizing at -35 °C overnight. Red crystals were isolated in 78% yield (78 mg). Anal. found (calcd) for $C_{23}H_{52}O_2P_4Fe$: C, 50.15

(51.12); H, 9.60 (9.70). Data for C analysis low even after multiple trials, possibly due to difficulties of handling air sensitive materials. Evidence of bulk purity given by NMR spectral figures in the Supporting Information. ^{1}H NMR (600 MHz, C_6D_6): δ 2.94 (ddd, 1H, *J* = 17.0, 11.1, 4.3 Hz, Fe-β-C*H*$_2$), 2.84 (ddd, 1H, *J* = 16.9, 11.0, 5.4 Hz, Fe-β-C*H*$_2$), 1.94 (m, 1H, Fe-α-C*H*$_2$), The signals for P-C*H*$_2$ and P-C*H*$_3$ of depe ligand were not suitably resolved to permit definitive assignment, 2.34 (m, 1H, PC*H*$_2$), 2.05 (m, 1H, PC*H*$_2$), 1.86 – 1.74 (m, 4H, PC*H*$_2$ & PC*H*$_3$), 1.74 – 1.56 (m, 3H, , PC*H*$_2$ & PC*H*$_3$), 1.56 – 1.47 (m, 3H, PC*H*$_2$ & PC*H*$_3$), 1.47 – 1.34 (m, 3H, , PC*H*$_2$ & PC*H*$_3$), 1.34 – 0.89 (m, 25H, PC*H*$_2$ & PC*H*$_3$, 1H corresponds to Fe-α-C*H*$_2$), 0.82 – 0.66 (m, 5H, PC*H*$_2$ & PC*H*$_3$), 0.56 (m, 4H, PC*H*$_2$ & PC*H*$_3$). ^{13}C {^{1}H} NMR (600 MHz, C_6D_6): δ 189.1 (d, *J* = 14.1 Hz, *C*=O), 37.8 (d, *J* = 4.1 Hz, Fe-β-*C*H$_2$), -2.1 (apparent quintet, *J* = 18.6 Hz, Fe-α-*C*H$_2$), following signals assigned as P-*C*H$_2$ and P-*C*H$_3$ of depe ligand: 25.0 (d, *J* = 12.7 Hz), 24.5 (ddd, *J* = 21.8, 15.9, 6.4 Hz), 24.3 (d, *J* = 10.8 Hz), 23.4 (t, *J* = 19.7 Hz), 22.7 (d, *J* = 6.0 Hz), 22.6 (m), 21.5 (d, *J* = 12.1 Hz), 20.2 (dd, *J* = 21.6, 14.1 Hz), 19.0 (d, *J* = 10.6 Hz), 18.6 (m), 13.1 (dd, *J* = 15.2, 10.0 Hz), 10.0 (d, *J* = 6.2 Hz), 9.4 (m), 9.2 (d, *J* = 7.6 Hz), 9.0 (d, *J* = 4.9 Hz), 8.3 (d, *J* = 4.8 Hz), 8.1 (d, *J* = 4.1 Hz), 8.0 (d, *J* = 6.5 Hz), two resonances assumed to correspond to coincident carbons. ^{31}P {^{1}H} NMR (C_6D_6): δ 80.12 (ddd, 1P, *J* = 8.5, 32.8, 37.7 Hz), 73.37 (ddd, 1P, *J* = 18.1, 37.5, 166.3 Hz), 71.50 (ddd. 1P, *J* = 25.7, 33.1, 166.6 Hz), 68.17 (ddd, 1P, *J* = 8.5, 19.4, 26.7 Hz). IR (KBr): $\upsilon_{C=O}$ = 1593 cm^{-1}.

Synthesis of *trans*-(depe)$_2$Fe(H)(κ*O*-O$_2$CCH=CH$_2$) (7). To a 20 mL Scintillation vial 137 mg (0.28 mmol) (depe)$_2$Fe(N$_2$) and 8 mL THF were added. 18.9 µL acrylic acid (0.28 mmol) was added dropwise via a micro-syringe. The reaction solution immediately changed from orange to yellow. Volatiles were removed in vacuo and the residue dissolved in pentane and filtered through a Pasture pipette. The filtrate was slightly condensed and recrystallized at -35 °C overnight. Yellow-orange solid was obtained in 56% yield (84 mg). Crystals suitable for x-ray diffraction were grown in pentane via slow evaporation at ambient temperature. Anal. found (calcd) for $C_{23}H_{52}O_2P_4Fe$: C, 50.22 (51.12); H, 9.65 (9.70). Data for C analysis low even after multiple trials, possibly due to difficulties of handling air sensitive materials. Evidence of bulk purity given by NMR spectral figures in the Supporting Information. ^{1}H NMR (600 MHz, C_6D_6): δ

6.26 (dd, 1H, J = 17.2, 10.0 Hz, $CO_2CH{=}CH_2$), 6.01 (dd, 1H, J = 17.2, 2.9 Hz. $CO_2CH{=}CH_2$), 5.20 (dd, 1H, J = 10.0, 3.1 Hz, $CO_2CH{=}CH_2$), -33.16 (p, J = 47.5 Hz, Fe-*H*), The signals for P-CH_2 and P-CH_3 of depe ligand were not suitably resolved to permit definitive assignment, 2.22 (m, 4H, J = 7.3 Hz), 2.13 (br s, 4H), 1.81 – 1.72 (m, 4H), 1.59 (h, 4H, J = 7.3 Hz), 1.51 (br s, 4H), 1.14 - 1.06 (m, 16H), 0.89 – 0.81 (m, 12H). ^{13}C {^1H} NMR (600 MHz, C_6D_6): δ 173.5 (s, *C*=O), 138.0 (s, $CO_2CH{=}CH_2$), 120.1 (s, $CO_2CH{=}CH_2$), following signals assigned as P-*C*H_2 and P-*C*H_3 of depe ligand: 23.6 (br s), 23.1 (p, J = 12.6 Hz), 20.8 (br s), 9.2 (s), 8.8 (s), multiple resonances assumed to correspond to coincident carbons. ^{31}P {^1H} NMR (300 MHz, C_6D_6): δ 89.95 (d, 4P, J = 44.3 Hz). IR (KBr): $\upsilon_{C=C}$ = 1632 cm^{-1}, $\upsilon_{C=O}$ = 1591 cm^{-1}.

Data for (depe)$_2$Fe(CO) (3): Additional characterization not previously reported: ^{13}C {^1H} NMR (600 MHz, C_6D_6): δ 224.5 (p, J = 10.5 Hz, *C*≡O), following signals assigned as P-*C*H_2 and P-*C*H_3 of depe ligand: 27.3 (br s), 26.9 (ddd, J = 25.9, 21.4, 3.7 Hz), 9.2 (s), multiple resonances assumed to correspond to coincident carbons.

Data for (depe)$_2$Fe(CO$_3$) (4). This complex was synthesized according to the previously reported procedure for the analogous dmpe complex (dmpe = 1,2-bis(dimethylphosphino)ethane) (dmpe)$_2$Fe(CO_3).[48] ^1H NMR (600 MHz, C_6D_6): δ 2.40 (m, 2H), 2.02 (m, 2H), 1.78 (m, 2H), 1.65 (m, 4H), 1.60 – 1.21 (m, 14H), 1.13 – 0.93 (m, 14H), 0.82 – 0.63 (m, 10H). ^{13}C {^1H} NMR (600 MHz, C_6D_6): δ 165.2 (s, *C*O_3), following signals assigned as P-*C*H_2 and P-*C*H_3 of depe ligand: 24.8 (d, J = 13.5 Hz), 23.6 (m), 20.7 (m), 19.7 (t, J = 6.3 Hz), 19.4 (m), 11.5 (t, J = 6.5 Hz), 9.4 (s), 9.0 (s), 8.6 (s), 7.7 (s), all resonances for depe ligand assumed to correspond to two coincident carbons. ^{31}P {^1H} NMR (300 MHz, C_6D_6): δ 80.54 (t, 2P, J = 35.0 Hz), 70.62 (t, 2P, J = 35.1 Hz).

Attempted Catalytic Acrylate Formation. In a typical trial, 0.1 mmol (depe)$_2$ Fe(C_2H_4), 20 mmol 2,6-diisopropyl sodium phenoxide, 5 mmol lithium triflate, 10 mmol zinc dust, and 25 mL tetrahydrofuran were added to a 100 mL Parr reactor glass insert. The reactor was charged with 28 bar ethylene and 2 bar carbon

dioxide before heating to 110 °C and stirring for 20 hours. The reaction was then cooled to room temperature before 50 mg of sorbic acid and 100 mg of sodium hydroxide were dissolved in deuterium oxide and added to the solution. Three extractions with diethyl ether were performed, and acrylate production was quantified by ^{1}H NMR integration against the sorbic acid standard in the deuterium oxide layer.

Oxalate Formation Experimental Method. In a typical trial, a 100 mL heavy walled glass reaction vessel was charged with 0.04 mmol $(depe)_2Fe(CO_2)$ and 0.8 mmol KC_8. Then 15 mL of THF was added via vacuum transfer on a high vacuum line. While keeping the flask cooled at -196 °C, 4.7 mmol (about 1.5 atm) carbon dioxide was added. The reaction was stirred for 8 hours at ambient temperature. The reaction was next filtered through Celite, followed by rinsing with 50 mL THF to remove any remaining organometallic material. The THF filtrate was discarded. The filter cake was then washed with 20 mL of 1 M HCl, followed by 60 mL water. The aqueous filtrate was pumped down on the rotary evaporator for 20 minutes to remove any residual THF, and the remaining aqueous solution titrated with 0.1 M potassium permanganate (standardized by titration of potassium oxalate monohydrate) to determine the total oxalate yield.[67]

Acknowledgements

This article is based upon work supported by the National Science Foundation (CHE-1955289) and the Curators of the Univ. of Missouri.

Associated Content

Supporting Information

The Supporting Information is available free of charge on the ACS Publications website at DOI: [to be inserted.]

Crystallographic Information Files (CDCC # 2021625 – 2021627)

Complete Catalytic Trial Data

Selected NMR Spectra

Cyclic Voltammograms

Additional Experiment Descriptions

Competing Financial Interests

The authors declare no competing financial interests.

References

(1) Burkart, M. D.; Hazari, N.; Tway, C. L.; Zeitler, E. L. Opportunities and Challenges for Catalysis in Carbon Dioxide Utilization. *ACS Catal.* **2019**, *9* (9), 7937–7956. https://doi.org/10.1021/acscatal.9b02113.

(2) Wang, W.; Wang, S.; Ma, X.; Gong, J. Recent Advances in Catalytic Hydrogenation of Carbon Dioxide. *Chem. Soc. Rev.* **2011**, *40* (7), 3703–3727. https://doi.org/10.1039/c1cs15008a.

(3) Costentin, C.; Robert, M.; Savéant, J. M. Catalysis of the Electrochemical Reduction of Carbon Dioxide. *Chemical Society Reviews*. 2013, pp 2423–2436. https://doi.org/10.1039/c2cs35360a.

(4) Laitar, D. S.; Müller, P.; Sadighi, J. P. Efficient Homogeneous Catalysis in the Reduction of CO2 to CO. *J. Am. Chem. Soc.* **2005**, *127* (49), 17196–17197.

https://doi.org/10.1021/ja0566679.

(5) Costentin, C.; Passard, G.; Robert, M.; Savéant, J. M. Ultraefficient Homogeneous Catalyst for the CO2-to-CO Electrochemical Conversion. *Proc. Natl. Acad. Sci. U. S. A.* **2014**, *111* (42), 14990–14994. https://doi.org/10.1073/pnas.1416697111.

(6) Tanaka, R.; Yamashita, M.; Nozaki, K. Catalytic Hydrogenation of Carbon Dioxide Using Ir(III)-Pincer Complexes. *J. Am. Chem. Soc.* **2009**, *131* (40), 14168–14169. https://doi.org/10.1021/ja903574e.

(7) Zhang, Y.; MacIntosh, A. D.; Wong, J. L.; Bielinski, E. A.; Williard, P. G.; Mercado, B. Q.; Hazari, N.; Bernskoetter, W. H. Iron Catalyzed CO2 Hydrogenation to Formate Enhanced by Lewis Acid Co-Catalysts. *Chem. Sci.* **2015**, *6* (7), 4291–4299. https://doi.org/10.1039/c5sc01467k.

(8) Schieweck, B. G.; Westhues, N. F.; Klankermayer, J. A Highly Active Non-Precious Transition Metal Catalyst for the Hydrogenation of Carbon Dioxide to Formates. *Chem. Sci.* **2019**, *10* (26), 6519–6523. https://doi.org/10.1039/c8sc05230a.

(9) Kar, S.; Kothandaraman, J.; Goeppert, A.; Prakash, G. K. S. Advances in Catalytic Homogeneous Hydrogenation of Carbon Dioxide to Methanol. *J. CO2 Util.* **2018**, *23* (December 2017), 212–218. https://doi.org/10.1016/j.jcou.2017.10.023.

(10) Tominaga, K.; Sasaki, Y.; Watanabe, T.; Saito, M. Homogeneous Hydrogenation of Carbon Dioxide to Methanol Catalyzed by Ruthenium Cluster Anions in the Presence of Halide Anions. *Bull. Chem. Soc. Jpn.* **1995**, *68* (10), 2837–2842. https://doi.org/10.1246/bcsj.68.2837.

(11) Schneidewind, J.; Adam, R.; Baumann, W.; Jackstell, R.; Beller, M. Low-Temperature Hydrogenation of Carbon Dioxide to Methanol with a Homogeneous Cobalt Catalyst. *Angew. Chemie - Int. Ed.* **2017**, *56* (7), 1890–1893. https://doi.org/10.1002/anie.201609077.

(12) Su, X.; Xu, J.; Liang, B.; Duan, H.; Hou, B.; Huang, Y. Catalytic Carbon Dioxide Hydrogenation to Methane: A Review of Recent Studies. *J. Energy Chem.* **2016**, *25* (4), 553–565. https://doi.org/10.1016/j.jechem.2016.03.009.

(13) Manthiram, K.; Beberwyck, B. J.; Alivisatos, A. P. Enhanced Electrochemical Methanation of Carbon Dioxide with a Dispersible Nanoscale Copper Catalyst. *J. Am. Chem. Soc.* **2014**, *136* (38), 13319–13325. https://doi.org/10.1021/ja5065284.

(14) Sun, X.; Kang, X.; Zhu, Q.; Ma, J.; Yang, G.; Liu, Z.; Han, B. Very Highly Efficient Reduction of CO2 to CH4 Using Metal-Free N-Doped Carbon Electrodes. *Chem. Sci.* **2016**, *7* (4), 2883–2887. https://doi.org/10.1039/c5sc04158a.

(15) Wang, J.; You, Z.; Zhang, Q.; Deng, W.; Wang, Y. Synthesis of Lower Olefins by Hydrogenation of Carbon Dioxide over Supported Iron Catalysts. *Catal. Today* **2013**, *215*, 186–193. https://doi.org/10.1016/j.cattod.2013.03.031.

(16) Satthawong, R.; Koizumi, N.; Song, C.; Prasassarakich, P. Light Olefin Synthesis from CO2 Hydrogenation over K-Promoted Fe-Co Bimetallic Catalysts. *Catal. Today* **2015**, *251*, 34–40. https://doi.org/10.1016/j.cattod.2015.01.011.

(17) Dinh, C. T.; Burdyny, T.; Kibria, G.; Seifitokaldani, A.; Gabardo, C. M.; Pelayo García De Arquer, F.; Kiani, A.; Edwards, J. P.; De Luna, P.; Bushuyev, O. S.; et al. CO2 Electroreduction to Ethylene via Hydroxide-Mediated Copper Catalysis at an Abrupt

Interface. *Science (80-.).* **2018**, *360* (6390), 783–787. https://doi.org/10.1126/science.aas9100.

(18) Gennaro, A.; Isse, A. A.; Savéant, J. M.; Severin, M. G.; Vianello, E. Homogeneous Electron Transfer Catalysis of the Electrochemical Reduction of Carbon Dioxide. Do Aromatic Anion Radicals React in an Outer-Sphere Manner? *J. Am. Chem. Soc.* **1996**, *118* (30), 7190–7196. https://doi.org/10.1021/ja960605o.

(19) Tanaka, K.; Kushi, Y.; Tsuge, K.; Toyohara, K.; Nishioka, T.; Isobe, K. Catalytic Generation of Oxalate through a Coupling Reaction of Two CO 2 Molecules Activated on [(Ir(η 5 -C 5 Me 5)) 2 (Ir(η 4 -C 5 Me 5)CH 2 CN)(μ 3 -S) 2]. *Inorg. Chem.* **1998**, *37* (1), 120–126. https://doi.org/10.1021/ic9702328.

(20) Rudolph, M.; Dautz, S.; Jager, E. G. Macrocyclic [N4/2-] Coordinated Nickel Complexes as Catalysts for the Formation of Oxalate by Electrochemical Reduction of Carbon Dioxide. *J. Am. Chem. Soc.* **2000**, *122* (44), 10821–10830. https://doi.org/10.1021/ja001254n.

(21) Angamuthu, R.; Byers, P.; Lutz, M.; Spek, A. L.; Bouwman, E. Electrocatalytic CO2 Conversion to Oxalate by a Copper Complex. *Science (80-.).* **2010**, *327* (5963), 313–315. https://doi.org/10.1126/science.1177981.

(22) Pokharel, U. R.; Fronczek, F. R.; Maverick, A. W. Reduction of Carbon Dioxide to Oxalate by a Binuclear Copper Complex. *Nat. Commun.* **2014**, *5* (1), 1–5. https://doi.org/10.1038/ncomms6883.

(23) Cook, B. J.; Di Francesco, G. N.; Abboud, K. A.; Murray, L. J. Countercations and Solvent Influence CO2 Reduction to Oxalate by Chalcogen-Bridged Tricopper

Cyclophanates. *J. Am. Chem. Soc.* **2018**, *140* (17), 5696–5700. https://doi.org/10.1021/jacs.8b02508.

(24) Wang, X.; Wang, H.; Sun, Y. Synthesis of Acrylic Acid Derivatives from CO2 and Ethylene. *Chem* **2017**, *3* (2), 211–228. https://doi.org/10.1016/j.chempr.2017.07.006.

(25) Jin, D.; Schmeier, T. J.; Williard, P. G.; Hazari, N.; Bernskoetter, W. H. Lewis Acid Induced β-Elimination from a Nickelalactone: Efforts toward Acrylate Production from CO2 and Ethylene. *Organometallics* **2013**, *32* (7), 2152–2159. https://doi.org/10.1021/om400025h.

(26) Stieber, S. C. E.; Huguet, N.; Kageyama, T.; Jevtovikj, I.; Ariyananda, P.; Gordillo, A.; Schunk, S. A.; Rominger, F.; Hofmann, P.; Limbach, M. Acrylate Formation from CO2 and Ethylene: Catalysis with Palladium and Mechanistic Insight. *Chem. Commun.* **2015**, *51* (54), 10907–10909. https://doi.org/10.1039/c5cc01932j.

(27) Manzini, S.; Cadu, A.; Schmidt, A. C.; Huguet, N.; Trapp, O.; Paciello, R.; Schaub, T. Enhanced Activity and Recyclability of Palladium Complexes in the Catalytic Synthesis of Sodium Acrylate from Carbon Dioxide and Ethylene. *ChemCatChem* **2017**, *9* (12), 2269–2274. https://doi.org/10.1002/cctc.201601150.

(28) Knopf, I.; Tofan, D.; Beetstra, D.; Al-Nezari, A.; Al-Bahily, K.; Cummins, C. C. A Family of Cis-Macrocyclic Diphosphines: Modular, Stereoselective Synthesis and Application in Catalytic CO2/Ethylene Coupling. *Chem. Sci.* **2017**, *8* (2), 1463–1468. https://doi.org/10.1039/c6sc03614g.

(29) Vavasori, A.; Calgaro, L.; Pietrobon, L.; Ronchin, L. The Coupling of Carbon Dioxide with Ethene to Produce Acrylic Acid Sodium Salt in One Pot by Using Ni(II) and Pd(II)-

Phosphine Complexes as Precatalysts. *Pure Appl. Chem.* **2018**, *90* (2), 315–326. https://doi.org/10.1515/pac-2017-0706.

(30) Hopkins, M. N.; Shimmei, K.; Uttley, K. B.; Bernskoetter, W. H. Synthesis and Reactivity of 1,2-Bis(Di- Iso-Propylphosphino)Benzene Nickel Complexes: A Study of Catalytic CO 2 -Ethylene Coupling. *Organometallics* **2018**, *37* (20), 3573–3580. https://doi.org/10.1021/acs.organomet.8b00260.

(31) Ito, T.; Takahashi, K.; Iwasawa, N. Reactivity of a Ruthenium(0) Complex Bearing a Tetradentate Phosphine Ligand: Applications to Catalytic Acrylate Salt Synthesis from Ethylene and CO2. *Organometallics* **2019**, *38* (2), 205–209. https://doi.org/10.1021/acs.organomet.8b00789.

(32) Uttley, K. B.; Shimmei, K.; Bernskoetter, W. H. Ancillary Ligand and Base Influences on Nickel-Catalyzed Coupling of CO2 and Ethylene to Acrylate. *Organometallics* **2020**, *39*, 1573–1579. https://doi.org/10.1021/acs.organomet.9b00708.

(33) Davis, I. S. R. E.; Sot, J. A. C.; Steudel, R.; Maude, H.; Hoberg, B. H.; Jenni, K.; Angermund, K. CC-Linkages of Ethene with CO2, on an Iron(o) Complex-Synthesis and Crystal Structure Analysis of I(PEt3)2Fe(C2H4)21. *Angew Chem. Inr Ed. Engl* **1987**, *93* (1981), 153–155.

(34) Rummelt, S. M.; Zhong, H.; Korobkov, I.; Chirik, P. J. Iron-Mediated Coupling of Carbon Dioxide and Ethylene: Macrocyclic Metallalactones Enable Access to Various Carboxylates. *J. Am. Chem. Soc.* **2018**, *140* (37), 11589–11593. https://doi.org/10.1021/jacs.8b07558.

(35) Francke, R.; Schille, B.; Roemelt, M. Homogeneously Catalyzed Electroreduction of

Carbon Dioxide - Methods, Mechanisms, and Catalysts. *Chem. Rev.* **2018**, *118* (9), 4631–4701. https://doi.org/10.1021/acs.chemrev.7b00459.

(36) Paris, A. R.; Bocarsly, A. B. High-Efficiency Conversion of CO 2 to Oxalate in Water Is Possible Using a Cr-Ga Oxide Electrocatalyst. *ACS Catal.* **2019**, *9* (3), 2324–2333. https://doi.org/10.1021/acscatal.8b04327.

(37) Lejkowski, M. L.; Lindner, R.; Kageyama, T.; Bódizs, G. É.; Plessow, P. N.; Müller, I. B.; Schäfer, A.; Rominger, F.; Hofmann, P.; Futter, C.; et al. The First Catalytic Synthesis of an Acrylate from CO2 and an Alkene-A Rational Approach. *Chem. - A Eur. J.* **2012**, *18* (44), 14017–14025. https://doi.org/10.1002/chem.201201757.

(38) Hoberg, H.; Schaefer, D. Nickel(0) Induzierte C-C Verknupfung Zwischen Alkenen Und Kohlendioxid. *J. Organomet. Chem.* **1982**, *236* (1982), C28–C30.

(39) Graham, D. C.; Mitchell, C.; Bruce, M. I.; Metha, G. F.; Bowie, J. H.; Buntine, M. A. Production of Acrylic Acid through Nickel-Mediated Coupling of Ethylene and Carbon Dioxide - A DFT Study. *Organometallics* **2007**, *26* (27), 6784–6792. https://doi.org/10.1021/om700592w.

(40) Takahashi, K.; Cho, K.; Iwai, A.; Ito, T.; Iwasawa, N. Development of N-Phosphinomethyl-Substituted NHC-Nickel(0) Complexes as Robust Catalysts for Acrylate Salt Synthesis from Ethylene and CO2. *Chem. - A Eur. J.* **2019**, *25* (59), 13504–13508. https://doi.org/10.1002/chem.201903625.

(41) Bernskoetter, W. H.; Tyler, B. T. Kinetics and Mechanism of Molybdenum-Mediated Acrylate Formation from Carbon Dioxide and Ethylene. *Organometallics* **2011**, *30* (3), 520–527. https://doi.org/10.1021/om100891m.

(42) Wolfe, J. M.; Bernskoetter, W. H. Reductive Functionalization of Carbon Dioxide to Methyl Acrylate at Zerovalent Tungsten. *Dalt. Trans.* **2012**, *41* (35), 10763–10768. https://doi.org/10.1039/c2dt31032e.

(43) Baker, M. V.; Field, L. D. Reaction of Ethylene with a Coordinatively Unsaturated Iron Complex, Fe(DEPE)2: Sp C-H Bond Activation without Prior Formation of a π-Complex. *J. Am. Chem. Soc.* **1986**, *108* (23), 7436–7438. https://doi.org/10.1021/ja00283a065.

(44) Hirano, M.; Akita, M.; Tani, K.; Kumagai, K.; Kasuga, N. C.; Fukuoka, A.; Komiya, S. Activation of Coordinated Carbon Dioxide in Fe(CO2)(Depe)2 by Group 14 Electrophiles. *Organometallics* **1997**, *16* (19), 4206–4213. https://doi.org/10.1021/om960743m.

(45) Hayter, R. G.; Chatt, J. Chatt and Hayter. 5507 1079. Some Hydrido-Complexes. *J. Chem. Soc.* **1961**, *5507*, 5507–5511.

(46) Komiya, S.; Akita, M.; Yoza, A.; Kasuga, N.; Fukuoka, A.; Kai, Y. Isolation of a Zerovalent Iron Dinitrogen Complex with 1,2- Bis(Diethylphosphino)Ethane Ligands. *J. Chem. Soc. Chem. Commun.* **1993**, *205* (9), 787–788. https://doi.org/10.1039/C39930000787.

(47) Field, L. D.; Hazari, N.; Li, H. L. Nitrogen Fixation Revisited on Iron(0) Dinitrogen Phosphine Complexes. *Inorg. Chem.* **2015**, *54* (10), 4768–4776. https://doi.org/10.1021/acs.inorgchem.5b00211.

(48) Allen, O. R.; Dalgarno, S. J.; Field, L. D.; Jensen, P.; Turnbull, A. J.; Willis, A. C. Addition of CO2 to Alkyl Iron Complexes, Fe(PP) 2Me2. *Organometallics* **2008**, *27* (9), 2092–2098. https://doi.org/10.1021/om800091a.

(49) Jurd, P. M.; Li, H. L.; Bhadbhade, M.; Field, L. D. Fe(0)-Mediated Reductive Disproportionation of CO 2. *Organometallics* **2020**, *39*, 2011–2018. https://doi.org/10.1021/acs.organomet.0c00175.

(50) Gibson, D. H. The Organometallic Chemistry of Carbon Dioxide. *Chem. Rev.* **1996**, *96* (6), 2063–2095. https://doi.org/10.1021/cr940212c.

(51) Klose, A.; Hesschenbrouck, J.; Solari, E.; Latronico, M.; Floriani, C.; Re, N.; Chiesi-Villa, A.; Rizzoli, C. The Metal-Carbon Multiple Bond in Iron(I)- and Iron(II)-Dibenzotetramethyltetra[14]Azaannulene: Carbene, Carbonyl, and Isocyanide Derivatives. *J. Organomet. Chem.* **1999**, *591* (1–2), 45–62. https://doi.org/10.1016/S0022-328X(99)00354-X.

(52) Baker, M. V; Field, L. D. Reaction of Ethylene with a Coordinatively Unsaturated Iron Complex, Fe(DEPE)2: Sp C-H Bond Activation without Prior Formation of a π-Complex. *J. Am. Chem. Soc.* **1986**, *108* (23), 7436–7438. https://doi.org/10.1021/ja00283a065.

(53) Chatt, J.; Duncanson, L. A. Olefin Co-Ordination Compounds. Part III. Infra-Red Spectra and Structure: Attempted Preparation of Acetylene Complexes. *J. Chem. Soc.* **1953**, No. Part I, 2939–2947. https://doi.org/10.1039/jr9530002939.

(54) Hoberg, H.; Jenni, K.; Krüger, C.; Raabe, E. CC-Kupplung von CO2 Und Butadien an Eisen(o)-Komplexen – Ein Neuer Weg Zu α,ω-Dicarbonsäuren. *Angew. Chemie* **1986**, *98* (9), 819–820. https://doi.org/10.1002/ange.19860980915.

(55) Jurd, P. M.; Li, H. L.; Bhadbhade, M.; Dalgarno, S. J.; Mcintosh, R. D.; Field, L. D. The Reaction of Iron Acetylides with Carbon Dioxide. *Organometallics* **2020**, *39*, 1580–1589. https://doi.org/10.1021/acs.organomet.9b00830.

(56) Jin, D.; Williard, P. G.; Hazari, N.; Bernskoetter, W. H. Effect of Sodium Cation on Metallacycle β-Hydride Elimination in CO2-Ethylene Coupling to Acrylates. *Chem. - A Eur. J.* **2014**, *20* (11), 3205–3211. https://doi.org/10.1002/chem.201304196.

(57) Huguet, N.; Jevtovikj, I.; Gordillo, A.; Lejkowski, M. L.; Lindner, R.; Bru, M.; Khalimon, A. Y.; Rominger, F.; Schunk, S. A.; Hofmann, P.; et al. Nickel-Catalyzed Direct Carboxylation of Olefins with CO2: One-Pot Synthesis of α,β-Unsaturated Carboxylic Acid Salts. *Chem. - A Eur. J.* **2014**, *20* (51), 16858–16862. https://doi.org/10.1002/chem.201405528.

(58) Takahashi, K.; Hirataka, Y.; Ito, T.; Iwasawa, N. Mechanistic Investigations of the Ruthenium-Catalyzed Synthesis of Acrylate Salt from Ethylene and CO2. *Organometallics* **2020**, *4*. https://doi.org/10.1021/acs.organomet.9b00659.

(59) Aresta, M.; Nobile, C. F.; Albano, V. G.; Forni, E.; Manassero, M. New Nickel-Carbon Dioxide Complex: Synthesis, Properties, and Crystallographic Characterization of (Carbon Dioxide)- Bis(Tricyclohexylphosphine)Nickel. *J. Chem. Soc. Chem. Commun.* **1975**, *03* (15), 636–637. https://doi.org/10.1039/C39750000636.

(60) Calabrese, J. C.; Herskovitz, T.; Kinney, J. B. Carbon Dioxide Coordination Chemistry. 5. The Preparation and Structure of Rh(H1-CO2)(Cl)(Diars)2. *Journal of the American Chemical Society*. 1983, pp 5914–5915. https://doi.org/10.1021/ja00356a033.

(61) Komiya, S.; Akita, M.; Kasuga, N.; Hirano, M.; Fukuoka, A. Synthesis, Structure and Reactions of a Carbon Dioxide Complex of Iron(0) Containing 1,2-Bis(Diethylphosphino)Ethane Ligands. *J. Chem. Soc. Chem. Commun.* **1994**, No. 9, 1115–1116. https://doi.org/10.1039/C39940001115.

(62) Anderson, J. S.; Iluc, V. M.; Hillhouse, G. L. Reactions of CO2 and CS2 with 1,2-Bis(Di-Tert -Butylphosphino)Ethane Complexes of Nickel(0) and Nickel(I). *Inorg. Chem.* **2010**, *49* (21), 10203–10207. https://doi.org/10.1021/ic101652e.

(63) Kim, Y. E.; Kim, J.; Lee, Y. Formation of a Nickel Carbon Dioxide Adduct and Its Transformation Mediated by a Lewis Acid. *Chem. Commun.* **2014**, *50* (78), 11458–11461. https://doi.org/10.1039/c4cc04800h.

(64) Chiou, T. W.; Tseng, Y. M.; Lu, T. Te; Weng, T. C.; Sokaras, D.; Ho, W. C.; Kuo, T. S.; Jang, L. Y.; Lee, J. F.; Liaw, W. F. [NIII]-Mediated Reductive Activation of CO2 Affording a Ni(K1-OCO) Complex. *Chem. Sci.* **2016**, *7* (6), 3640–3644. https://doi.org/10.1039/c5sc04652a.

(65) Benson, E. E.; Kubiak, C. P.; Sathrum, A. J.; Smieja, J. M. Electrocatalytic and Homogeneous Approaches to Conversion of CO2 to Liquid Fuels. *Chem. Soc. Rev.* **2009**, *38* (1), 89–99. https://doi.org/10.1039/b804323j.

(66) Saouma, C. T.; Day, M. W.; Peters, J. C. CO2 Reduction by Fe(i): Solvent Control of C–O Cleavage versus C–C Coupling. *Chem. Sci.* **2013**, *4* (10), 4042–4051. https://doi.org/10.1039/c3sc51262b.

(67) Fowler, R. M.; Bright, H. A. Standardization of Permanganate Solutions with Sodium Oxalate. *J. Res. Natl. Bur. Stand. (1934).* **1935**, *15* (5), 493. https://doi.org/10.6028/jres.015.032.

(68) Michel, J. A.; Robinson, V. S.; Yang, L.; Sambandam, S.; Lu, W.; Westover, T.; Fisher, T. S.; Lukehart, C. M. Synthesis and Characterization of Potassium Metal/Graphitic Carbon Nanofiber Intercalates. *J. Nanosci. Nanotechnol.* **2008**, *8* (4), 1942–1950.

https://doi.org/10.1166/jnn.2008.308.

(69) Pangborn, A. B.; Giardello, M. A.; Grubbs, R. H.; Rosen, R. K.; Timmers, F. J. Safe and Convenient Procedure for Solvent Purification. *Organometallics* **1996**, *15* (5), 1518–1520. https://doi.org/10.1021/om9503712.

(70) Aranzaes, J. R.; Daniel, M. C.; Astruc, D. Metallocenes as References for the Determination of Redox Potentials by Cyclic Voltammetry - Permethylated Iron and Cobalt Sandwich Complexes, Inhibition by Polyamine Dendrimers, and the Role of Hydroxy-Containing Ferrocenes. *Can. J. Chem.* **2006**, *84* (2), 288–299. https://doi.org/10.1139/V05-262.

For Table of Contents Use Only